JOC Article

[2 + 4] and [4 + 2] Cycloadditions of *o*-Thioquinones with 1,3-Dienes: A Computational Study

Alessandro Contini,*,† Samantha Leone,† Stefano Menichetti,*,‡ Caterina Viglianisi,‡ and Pasqualina Trimarco†

Istituto di Chimica Organica "Alessandro Marchesini", Facoltà di Farmacia, Università degli Studi di Milano, via Venezian 21, 20133 Milano, Italy, and Dipartimento di Chimica Organica "Ugo Schiff" e Laboratorio di Progettazione Sintesi e Studio di Eterocicli Bioattivi (HeteroBioLab), Polo Scientifico Università degli Studi di Firenze, via della Lastruccia 13, I-50019 Sesto Fiorentino, Italy

alessandro.contini@unimi.it

Received March 2, 2006

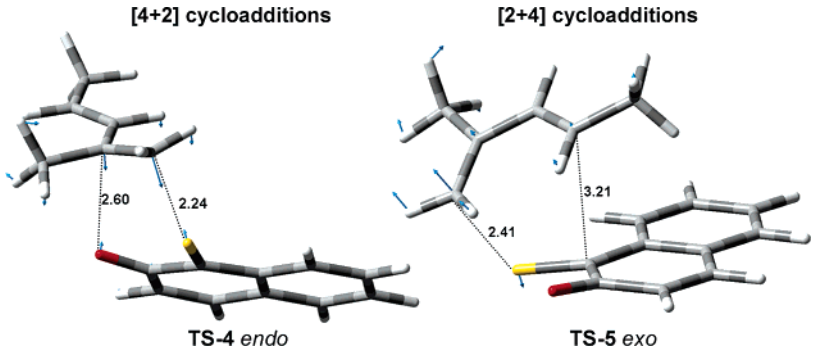

Cycloadditions of *o*-thioquinones (*o*-TQs) with 1,3-dienes could proceed via either a [2 + 4] or a [4 + 2] mechanism. Under kinetic control and with acyclic dienes the reaction affords the spiro cycloadducts **5** deriving from the [2 + 4] path as the main products. Under thermodynamic control, or with cyclic dienes, the *o*-TQs behave as heterodienes to give the benzoxathiin derivatives **4**, in most cases with complete regioselectivity. In the present computational study, DFT calculations were performed in order to achieve a deep understanding of both [2 + 4] and [4 + 2] paths. The reactions of three *o*-TQs with six 1,3-dienes were thoroughly investigated at the B3LYP/TZVP//B3LYP6-31G* level, and the two reaction mechanisms were then compared, evidencing that [2 + 4] cycloadditions are kinetically favored, strongly asynchronous, or even unconcerted, while [4 + 2] reactions are thermodynamically favored, quite asynchronous, but undoubtedly concerted. Moreover, the observed regioselectivity was rationalized by mean of the FMO theory and by comparison of the activation energies for different pathways.

Introduction

o-Thioquinones (*o*-TQs) are short-lived reactive species that can be generated in situ under mild conditions and reacted with electron-rich alkenes, including glycals and styrenes, in inverse electron-demand Diels−Alder reactions leading to the benzoxathiin cycloadducts **4** (Scheme 1).[1−3]

SCHEME 1

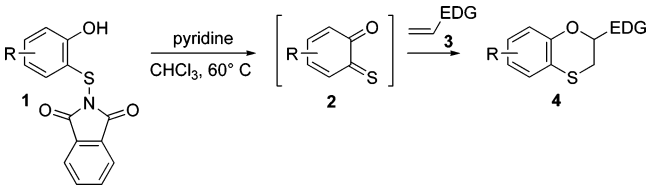

It was also reported that the carbon−sulfur double bond of the *o*-TQ **2a**, generated from the corresponding phthalimido derivative **1a**, could be trapped as a dienophile in the presence of 2,3-dimethyl-1,3-butadiene **3a**, leading to the formation of the spiro derivative **5aa**, as depicted in Scheme 2.[4]

However, Nair and co-workers recently published a series of articles describing the reaction of *o*-TQs **2**, generated from

* Corresponding author. Tel.: +390250314480. Fax: +390250314476.
† Università degli Studi di Milano.
‡ Università degli Studi di Firenze.

(1) Capozzi, G.; Falciani, C.; Menichetti, S.; Nativi, C. *J. Org. Chem.* **1997**, *62*, 2611−2615.
(2) Capozzi, G.; Falciani, C.; Menichetti, S.; Nativi, C.; Raffaelli, B. *Chem. Eur. J.* **1999**, 1748−1754.
(3) Capozzi, G.; Lo Nostro, P.; Menichetti, S.; Nativi, C.; Sarri, P. *Chem. Commun.* **2001**, 551−552.

10.1021/jo0604538 CCC: $33.50
Published on Web 06/20/2006

SCHEME 2

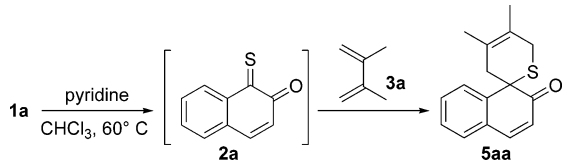

SCHEME 3. Possible Reaction Paths for the Cycloaddition of *o*-TQs 2 and 1,3-dienes

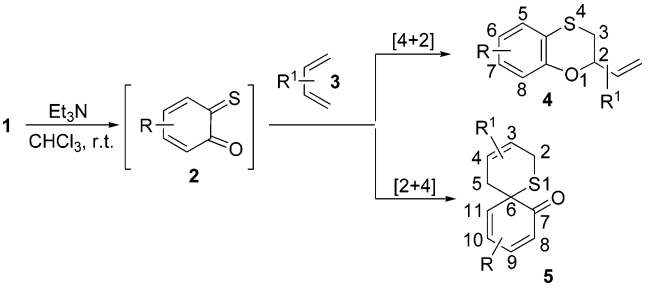

thiophthalimides **1** with a slightly modified procedure,[5] with acyclic and cyclic 1,3-dienes to assess the formation of the oxathiin derivatives **4** as the only cycloaddition products obtained via the participation of the oxothione moiety as a heterodiene.[6−10] Nevertheless, the possibility for *o*-TQs to participate as either heterodienes or dienophiles in cycloaddition reactions with 1,3-dienes, according to Scheme 3, was recently demonstrated for three different *o*-TQs generated under milder conditions (i.e. using Et_3N as a base in $CHCl_3$ at room temperature) and reacted with a series of both cyclic and acyclic 1,3-dienes, as represented in Figure 1.[11]

The analysis of the available experimental results led to the hypothesis that the [2 + 4] path, leading to the formation of the spiro derivatives **5**, was kinetically favored, but [4 + 2] products were thermodynamically more stable. However, some questions remained unsolved; indeed, it was not clear why the spiro derivatives where never obtained with cyclic dienes **3d**−**f**. Moreover, [4 + 2] products deriving from the reaction of o-TQs **2a,b** with dienes **3a,b** were not isolated in the adopted reaction conditions, even though a very small amount of **4ba** was detected by ^{1}H NMR when the spiro derivative **5ba** was heated for 70 h at 60 °C in $CDCl_3$, while **5aa** was stable under the same conditions for more than 240 h.[11] Furthermore, theoretical questions arose from the strong regioselectivity observed for [4 + 2] reactions when compared with the absence of regioselectivity of [2 + 4] cycloadditions; thus, the need of an exhaustive theoretical investigation on the reactivity of o-TQs toward 1,3-dienes was demonstrated. Indeed, the Diels−Alder and hetero Diels−Alder reaction mechanism has been the subject of debate since its discovery,[12−19] and the question of whether and when the [2 + 4] and the [4 + 2] cycloadditions herein described follow a concerted synchronous or asynchronous reaction mechanism could be considered of general interest. Furthermore, we recently reported a synthetic route involving the [4 + 2] cycloaddition of *o*-TQs leading to several polyhydroxylated 4-thiaflavans.[20] Such compounds are able to behave in vitro as very potent antioxidants, mimicking the action of flavonoids and/or tocopherols, and those encouraging results provided more impetus to our research, leading to the theoretical study here reported.

Computational Methods

Reactants, transition states (TSs), and products were completely optimized in the gas-phase using the B3LYP functional and the 6-31G(d) basis set.[21−23] Whenever a structure presented one or more degrees of freedom, several conformations were optimized, but only the most favored ones were further considered. Vibrational frequencies were computed at the same level of theory in order to define optimized geometries as either minima (no imaginary frequencies) or transition states (one imaginary frequency corresponding to the vibrational stretching of the forming bonds) and to calculate ZPVE corrections to electronic energies and thermochemical corrections to enthalpies and Gibbs free energies (unscaled, 298.15 K, 1 atm). For greater accuracy and to quantify the dependence of the energetic results from the employed basis set, single point energies were computed for all the stationary points at the B3LYP/TZVP level.[24] The triple split valence TZVP basis set was chosen because in our previous works it provided very good accuracy at a reasonable computational cost.[25] Total energies of the reactants derive from the sum of the isolated reactants energies, acyclic dienes **3a**−**c** were considered in the more stable *s*-trans conformation. To verify if the gas-phase model was reliable enough to correctly describe the behavior of both the [4 + 2] and [2 + 4] cycloadditions, reactants **2a** and **3c**, products **4ac** and **5ac**, transition states **TS-4ac**, **TS-5ac**, and **TS2-5ac**, and the intermediate **I-5ac** were reoptimized in solution by adopting the PCM model for $CHCl_3$ at the B3LYP/6-31G(d) level,[26] while single point energies were computed using the TZVP basis set. Results were then compared with those obtained in the gas phase, and only slightly different activation and reaction energies were observed, while no relevant differences were obtained upon the optimized geometries and reaction mechanism features, confirming the gas-phase model as accurate enough for our purposes. It was argued that the adequate description of the geometry

(4) Capozzi, G.; Dios, A.; Franck, R. W.; Geer, A.; Marzabaldi, C.; Menichetti, S.; Nativi, C.; Tamarez, M. *Angew. Chem., Int. Ed. Engl.* **1996**, *35*, 777−779.
(5) Reaction conditions: pyridine, $CHCl_3$, sealed tube, 70 °C.
(6) Nair, V.; Mathew, B.; Radharkrishnan, K. V.; Rath, N. P. *Synlett* **2000**, 61−62.
(7) Nair, V.; Mathew, B. *Tetrahedron Lett.* **2000**, *41*, 6919−6921.
(8) Nair, V.; Mathew, B.; Thomas, S.; Vairamani, M.; Prabhakar, S. *J. Chem. Soc., Perkin Trans. 1* **2001**, 3020−3024.
(9) Nair, V.; Mathew, B.; Rath, N. P.; Vairamani, M.; Prabhakar, S. *Tetrahedron* **2001**, *57*, 8349−8356.
(10) Nair, V.; Mathew, B.; Menon, R. S.; Mathew, S.; Vairamani, M.; Prabhakar, S. *Tetrahedron* **2002**, *58*, 3235−3241.
(11) Menichetti, S.; Viglianisi, C. *Tetrahedron* **2003**, *59*, 5523−5530.
(12) Dewar, M. J.; Olivella, S.; Stewart, J. J. *J. Am. Chem. Soc.* **1986**, *108*, 5771−5779.
(13) Trân huu Dâu, M. E.; Flament, J.-P.; Lefour, J.-M.; Riche, C.; Grierson, D. S.; *Tetrahedron Lett.* **1992**, *33*, 2343−2346.
(14) Coxon, J. M.; McDonald, D. Q. *Tetrahedron Lett.* **1992**, *33*, 3673−3676.
(15) Houk, K. N.; Gonza, W. J.; Li, Y. *Acc. Chem. Res.* **1995**, *28*, 81−90.
(16) Domingo, L. R.; Arnó, M.; Andrés, J. *J. Org. Chem.* **1999**, *64*, 5867−5875.
(17) Manoharan, M.; Proft, F. D.; Geerlings, P. *J. Org. Chem.* **2000**, *65*, 7971−7976.
(18) Wang, H.; Wang, Y.; Han, K.; Peng, X. *J. Org. Chem.* **2005**, *70*, 4910−4917.
(19) Paddon-Row: M. N.; Moran, D.; Jones, G. A.; Sherburn, M. S. *J. Org. Chem.* **2005**, *70*, 10841−10853.
(20) Menichetti, S.; Aversa, M. C.; Cimino, F.; Contini, A.; Viglianisi, C.; Tomaino, A. *Org. Biomol. Chem.* **2005**, *3*, 3066−3072.
(21) Lee, C.; Yang, W.; Parr, R. G. *Phys. Rev. B* **1988**, *37*, 785−789.
(22) Becke, A. D., *J. Chem. Phys.* **1993**, *98*, 5648−5652.
(23) Frisch, M. J.; Pople, J. A.; Binkley, J. S. *J. Chem. Phys.* **1984**, *80*, 3265−3269.
(24) Schäfer, A.; Huber, C.; Ahlrichs, R. *J. Chem. Phys.* **1994**, *100*, 5829−5835.
(25) Contini, A.; Nava, D.; Trimarco, P. *J. Org. Chem.* **2006**, *71*, 159−166.
(26) Cammi, R.; Mennucci, B.; Tomasi, J. *J. Phys. Chem. A* **2000**, *104*, 5631−5637.

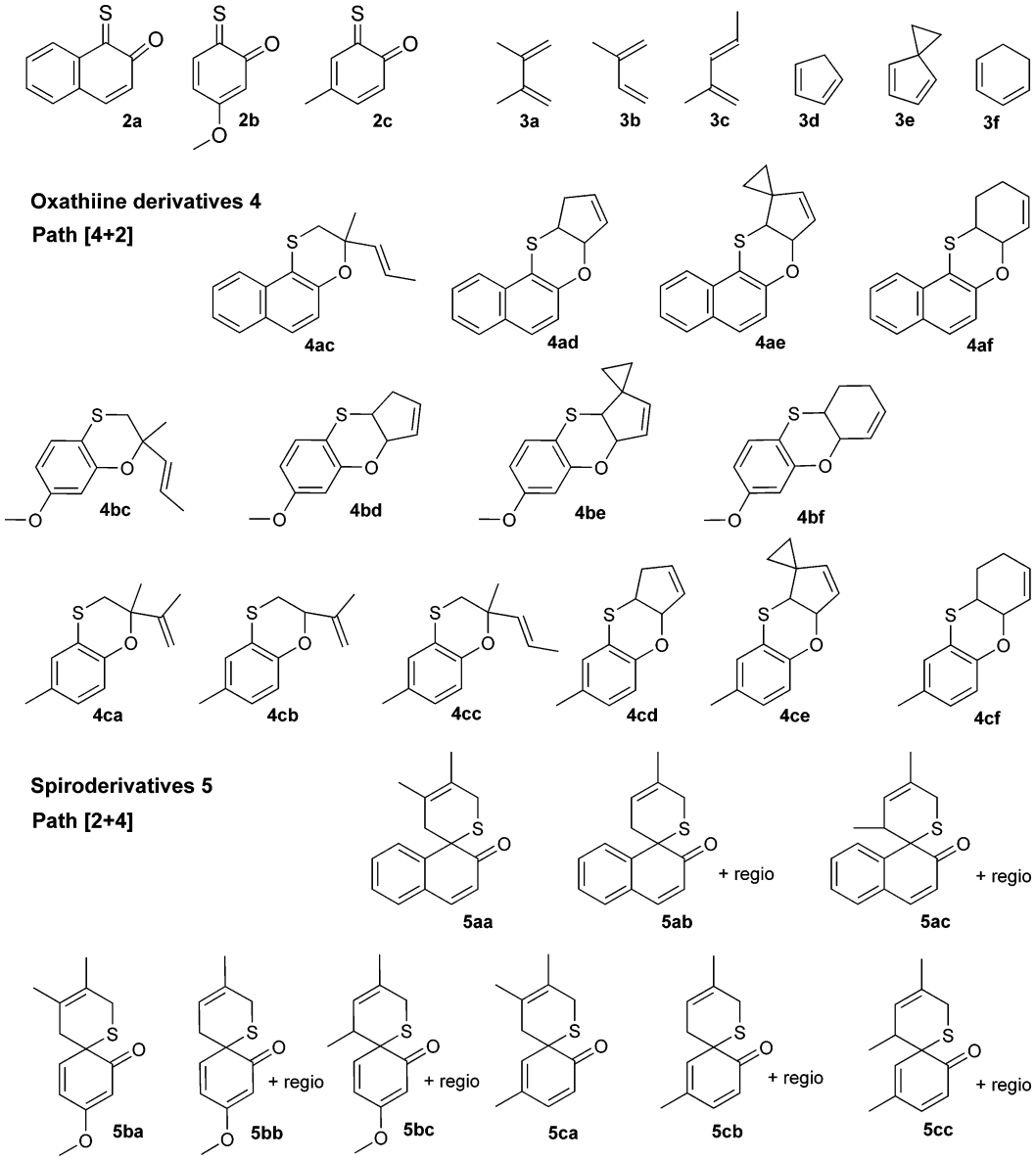

FIGURE 1. Reactants and experimentally observed products from [4 + 2] and [2 + 4] reaction paths.

and electronic properties of sulfur-containing compounds would require the inclusion of supplementary d functions in the basis set.[27,28] The model reactions of **2a** and **3c** were then thoroughly reanalyzed by using the 6-31G(d,p) basis set with additional 2df functions on the S atom, but comparable results were obtained, and thus our choice for geometry optimizations remains the simpler 6-31G(d) (additional details in the Supporting Information). To exclude a competing biradicalic pathway for [2 + 4] cycloadditions, the RHF−UHF stability of the wave function was checked for **TS-5ac** and **TS2-5ac**, but both RB3LYP and UB3LYP methods provided the same energy, and no instabilities were observed. IRC analyses were performed at the B3LYP/6-31G(d) level for both the endo and exo approaches of the [4 + 2] and [2 + 4] reaction paths for the cycloadditions of *o*-TQ **2a** with 1,3-diene **3c**, requesting in each case a step size of 0.1 amu$^{1/2}$ bohr. All theoretical calculations were performed with the Gaussian 03 program package.[29] Cartesian coordinates and energies for the obtained stationary points are supplied as Supporting Information.

Results and Discussion

The discussion hereafter reported is based upon the optimization of nine reactants (*o*-TQs **2a**−**c** and 1,3-dienes **3a**−**d**), 62

(27) Juaristi, E.; Notario, R.; Roux, M. V. *Chem. Soc. Rev.* **2005**, *34*, 347−354.

(28) Roux, M. V.; Temprado, M.; Jimènez, P.; Dávalos, J. Z.; Notario, R.; Martín-Valcárel G.; Garrido, L.; Guzmán-Mejía R.; Juaristi, E. *J. Org. Chem*. **2004**, *69*, 5454−5459.

(29) Frisch, M. J.; Trucks, G. W.; Schlegel, H. B.; Scuseria, G. E.; Robb, M. A.; Cheeseman, J. R.; Montgomery, Jr., J. A.; Vreven, T.; Kudin, K. N.; Burant, J. C.; Millam, J. M.; Iyengar, S. S.; Tomasi, J.; Barone, V.; Mennucci, B.; Cossi, M.; Scalmani, G.; Rega, N.; Petersson, G. A.; Nakatsuji, H.; Hada, M.; Ehara, M.; Toyota, K.; Fukuda, R.; Hasegawa, J.; Ishida, M.; Nakajima, T.; Honda, Y.; Kitao, O.; Nakai, H.; Klene, M.; Li, X.; Knox, J. E.; Hratchian, H. P.; Cross, J. B.; Adamo, C.; Jaramillo, J.; Gomperts, R.; Stratmann, R. E.; Yazyev, O.; Austin, A. J.; Cammi, R.; Pomelli, C.; Ochterski, J. W.; Ayala, P. Y.; Morokuma, K.; Voth, G. A.; Salvador, P.; Dannenberg, J. J.; Zakrzewski, V. G.; Dapprich, S.; Daniels, A. D.; Strain, M. C.; Farkas, O.; Malick, D. K.; Rabuck, A. D.; Raghavachari, K.; Foresman, J. B.; Ortiz, J. V.; Cui, Q.; Baboul, A. G.; Clifford, S.; Cioslowski, J.; Stefanov, B. B.; Liu, G.; Liashenko, A.; Piskorz, P.; Komaromi, I.; Martin, R. L.; Fox, D. J.; Keith, T.; Al-Laham, M. A.; Peng, C. Y.; Nanayakkara, A.; Challacombe, M.; Gill, P. M. W.; Johnson, B.; Chen, W.; Wong, M. W.; Gonzalez, C.; Pople, J. A. *Gaussian 03*, Revision B.04; Gaussian, Inc.: Pittsburgh, PA, 2003.

TABLE 1. Activation and Reaction Enthalpies and Gibbs Free Energies ($\Delta H^{\ddagger}$, $\Delta G^{\ddagger}$ and ΔH, ΔG, kcal/mol) for [4 + 2] and [2 + 4] Reactions of *o*-TQs 2a-c with 1,3-Dienes 3a−f[a,b]

[4 + 2]					[2 + 4]				
entry	$\Delta H^{\ddagger}$	$\Delta G^{\ddagger}$	ΔH	ΔG	entry	$\Delta H^{\ddagger}$	$\Delta G^{\ddagger}$	ΔH	ΔG
4aa[c,e]	9.2	23.0	−24.8	−9.0	**5aa**	5.0	18.7	−18.5	−3.5
4ab[c]	9.3	23.0	−24.0	−8.4	**5ab**	5.0	18.6	−18.9	−4.0
4ac	8.2	21.4	−24.9	−9.2	**5ac**[f]	3.5	17.0	−14.3	1.6
4ad	5.4	19.6	−23.6	−7.9	**5ad**[c]	4.3	19.7	−3.0	12.8
4ae	6.3	20.9	−22.2	−6.3	**5ae**[c]	8.6	24.5	−0.7	15.7
4af	6.8	21.1	−26.8	−11.6	**5af**[c]	6.6	21.9	−9.1	6.8
4ba[d]	7.4	20.6	−27.8	−12.5	**5ba**	3.3	15.6	−21.0	−6.6
4bb[c]	7.6	20.5	−27.1	−12.2	**5bb**	3.2	16.0	−20.8	−6.2
4bc	6.4	18.8	−28.0	−12.9	**5bc**[f,g]	*h*		−17.1	−1.9
4bd	3.6	17.2	−27.0	−12.0	**5bd**[c]	3.3	18.2	−10.0	5.3
4be	3.9	17.7	−25.7	−10.4	**5be**[c]	8.0	23.1	−3.8	11.8
4bf	5.6	18.8	−29.8	−15.2	**5bf**[c]	5.5	20.1	−11.7	3.1
4ca[e]	6.9	19.8	−31.1	−17.0	**5ca**[f]	3.7	16.1	−18.6	−4.3
4cb	7.0	19.4	−31.3	−16.9	**5cb**	3.6	16.1	−18.5	−3.9
4cc	5.9	18.1	−31.4	−17.0	**5cc**[f,g]	*h*		−14.8	0.5
4cd	3.2	16.5	−30.2	−15.6	**5cd**[c]	3.8	18.8	−7.6	7.4
4ce	3.5	16.9	−28.8	−14.1	**5ce**[c]	8.6	23.8	−1.8	13.7
4cf	4.8	17.7	−34.0	−18.3	**5cf**[c]	5.6	20.1	−9.4	5.6

[a] Calculated as the sum of B3LYP/TZVP energy and the thermal correction to enthalpy or Gibbs free energy obtained from thermochemical calculations (298.15 K, 1 atm) at the B3LYP/6-31G(d) level. Activation barriers are calculated as the energy difference between TSs and the sum of the isolated reactants energies, while reaction energies correspond to the energy differences between products and the sum of the isolated reactants energies. [b] R1 regioisomers were considered for both [4 + 2] and [2 + 4] reactions. [c] Those products were never experimentally observed. [d] Product **4ba** was never isolated; however, very small amounts of **4ba** were detected by ^{1}H NMR when **5ba** was heated for 70 h at 60 °C in $CDCl_3$. Under the same conditions, **5aa** was stable for more than 240 h. [e] Contrarily to what generally observed for [4 + 2] reactions, in those cases the exo TS results were slightly favored. [f] Those products were never isolated; however, they where detected by ^{1}H NMR. [g] **TS-5bc** and **TS-5cc** did not converge. [h] Not converged.

products, and 86 different transition structures, corresponding to the approaches of *o*-TQs **2a**−**c** to 1,3-dienes **3a**−**f** for both the [4 + 2] and [2 + 4] reaction paths, including TSs leading to allowed but not experimentally observed products and/or regioisomers, together with endo- and exo-TSs that, due to the symmetric nature of dienes **3a,b,d**−**f**, would lead to the same product. Thus, in the following sections, we will discuss the reasons concerning the [4 + 2] or [2 + 4] selectivity, provide details on both reaction mechanism, and discuss the observed regioselectivity. All the stationary points geometries and the corresponding energies are available as Supporting Information.

[4 + 2] vs [2 + 4]: Activation Barriers and Reaction Energies. Concerning the cycloadditions of *o*-TQs **2a**−**c** with acyclic dienes **3a**−**c**, activation barriers reported in Table 1 show that the [2 + 4] reaction path is kinetically favored. Indeed, the activation enthalpies $\Delta H^{\ddagger}$ were from 3.2 (**2c** + **3a**) to 4.7 (**2a** + **3c**) lower than those observed for the corresponding [4 + 2] paths. Instead, [4 + 2] reactions were decidedly favored from the thermodynamic point of view as, in terms of reaction enthalpies ΔH, oxathiin derivatives **4** are from 5.1 (**4ab**) to 16.6 kcal/mol (**4cc**) more stable than the corresponding spiro derivatives **5**. Cyclic dienes **3d**−**e**, on the other hand, show a marked preference for [4 + 2] reactions. Indeed, activation enthalpies of [2 + 4]s are lower than those calculated for [4 + 2]s only for reactions of *o*-TQs **2a,b** with dienes **3d,f** (from 0.1 to 1.1 kcal/mol for **2b** + **3f** and **2a** + **3d**, respectively), while [4 + 2] cycloadditions were kinetically favored in the other cases. Moreover, reaction enthalpies show that [4 + 2] products are from 17.0 (**4bd**) to 27.0 (**4be**) kcal/mol more stable

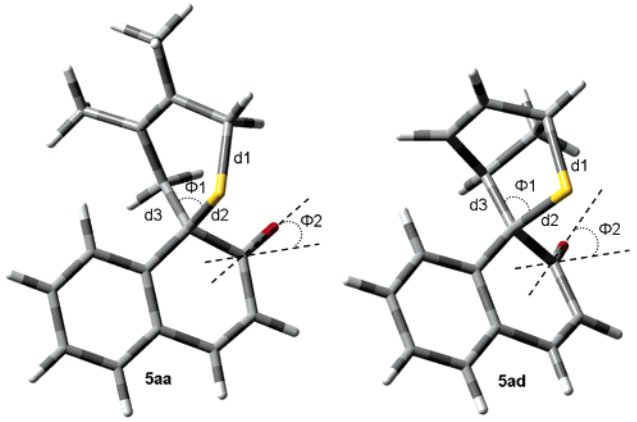

FIGURE 2. Products **5aa** (left) and **5ad** (right) from the [2 + 4] cycloadditions of *o*-TQ **2a** with dienes **3c** and **3d**, respectively. Selected geometrical parameters (Å, deg) for **5aa** and, in parentheses, for **5ad**: d1 = 1.84 (1.89), d2 = 1.88 (1.92), d3 = 1.57 (1.59), Φ_1 = 111.9 (102.3), Φ_2 = 9.1 (18.3).

than the corresponding [2 + 4] products, thus leading to the conclusion that the spiro derivatives **5** could not be obtained from cyclic dienes. Such results fit perfectly with the reported experimental outcome of [4 + 2] and [2 + 4] cycloadditions of *o*-TQs.[11]

As shown in Figure 2, the reason for the observed thermodynamic instability of [2 + 4] products deriving from cyclic dienes **3d**−**f** can be due to the structural strain induced by the spiro bicyclical moiety, as deduced from the longer S1−C2, S1−C6, and C5−C6 distances (d1, d2 and d3, respectively, in Figure 2), the unfavorable S1−C6−C5 sp^3 angle, and the considerable distortion of the carbonyl respect to the ring plane (Φ_1 and Φ_2, respectively, in Figure 2), if compared with the thermodynamically stable spiro derivatives obtained from acyclic dienes. Such observation is confirmed by the relatively more favorable energies obtained for the less strained spiro compounds deriving from cycloesadiene **3f**, if compared with those deriving from cyclopentadienes **3d** and **3e** (see Table 1). Interestingly, the analysis of activation energies reported in Table 1 show that the reactivity of *o*-TQs **2a**−**c** toward [4 + 2] cycloadditions decrease in the order **2c** > **2b** > **2a**, as $\Delta H^{\ddagger}$ values were from 3.2 to 7.0 kcal/mol for the former, from 3.6 to 7.6 kcal/mol for the second, and from 5.4 to 9.3 for the latter. In each case, the cyclopentadiene **3d** was the most reactive 1,3-diene, while the 2-methylbutadiene **3b** was the least reactive. On the other hand, concerning [2 + 4] cycloadditions, the reactivity order is less marked, with $\Delta H^{\ddagger}$ values ranging from 3.2 to 8.0 kcal/mol for *o*-TQ **2b**, from 3.5 to 8.6 kcal/mol for **2a**, and from 3.6 to 8.6 kcal/mol for **2c**. The 2-methylpenta-1,3-diene **3c** was the most reactive with *o*-TQ **2a**, but unfortunately, transition states **TS-5bc** and **TS-5cc** did not fully converge, neither in gas phase nor in solvent, probably because of the marked flatness of the PES in the region where **TS-5bc** and **TS-5cc** should lie. However, due to the good comparability of the $\Delta H^{\ddagger}$ and $\Delta G^{\ddagger}$ values observed among all the other reactions of *o*-TQs **2a**−**c** with dienes **3a**−**f**, we could reasonably deduce that the diene **3c** was in each case the most reactive, while, for the above-discussed reasons, cyclopentadiene **3e** was the least reactive toward [2 + 4] cycloadditions. Finally, it should also be noted that cycloadditions of *o*-TQs **2a,b** with dienes **3a,b**, conduced at room temperature, did not afford the [4 + 2] products **4**, while *o*-TQ **3c** provided the oxathiines **4** with all the reacted dienes.[11] Indeed, results reported in Table

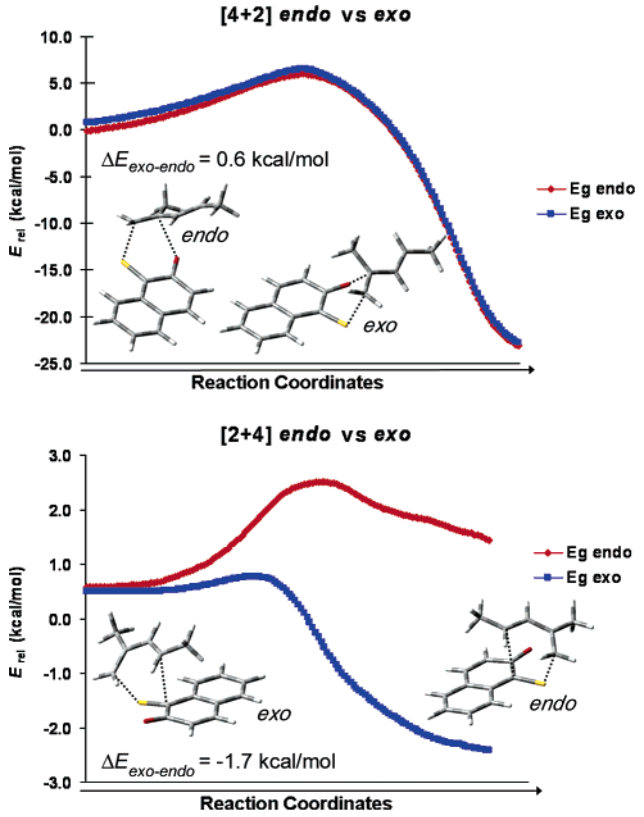

FIGURE 3. B3LYP/6-31G* IRC analyses of the endo and exo approaches for the [4 + 2] and [2 + 4] cycloadditions of *o*-TQ **2a** with diene **3c**.

1 show that the $\Delta\Delta G_{4-5}$ values are relatively low for **aa**, **ab**, **ba**, and **bb** (−5.5, −4.4, −5.9, and −6.0 kcal/mol, respectively) if compared with those calculated for products **ca** and **cb** (−12.7 and −13.0 kcal/mol, respectively), in concordance with the observed outcome of the reaction and thus providing a further validation to the adopted theoretical model.

Details of the Reaction Mechanism. The energetic values obtained for all the endo- and exo-TSs for [2 + 4] and [4 + 2] reactions (see Supporting Information), together with the IRC analyses reported in Figure 3 show that for [4 + 2] cycloadditions the endo approach is generally favored, unless differently specified, while for all [2 + 4] reactions the exo approach is decidedly preferred. For those reasons the following discussion will refer to the endo [4 + 2] and exo [2 + 4] TSs.

In terms of reaction mechanism, a quite evident diversity that can be observed between [4 + 2] and [2 + 4] TSs concern synchronicity. In a recent article, Peng et al. defined the synchronicity degree as the difference between the distances of the bonds that are being formed.[18] However, as the difference between the lengths of the fully formed C−S and C−O bonds is quite considerable (about 1.8 and 1.4 Å, respectively), we considered the synchronicity as the difference between the ratios of the forming bond distances in the TS and the corresponding bond distances in the product, i.e., $\Delta d_{TS/P} = |(C3-S4)_{TS}/(C3-S4)_p - (O1-C2)_{TS}/(O1-C2)_p|$ for [4 + 2] reactions and $\Delta d_{TS/P} = |(S1-C2)_{TS}/(S1-C2)_p - (C5-C6)_{TS}/(C5-C6)_p|$ for [2 + 4]s. Evidently, in the case of a totally synchronous reaction the $\Delta d_{TS/P}$ value is 0. Taking into account the above observations, the analysis of the geometrical parameters reported in Table S3 of the Supporting Information (selected distances for the cycloaddition products are reported in Table S4 of the

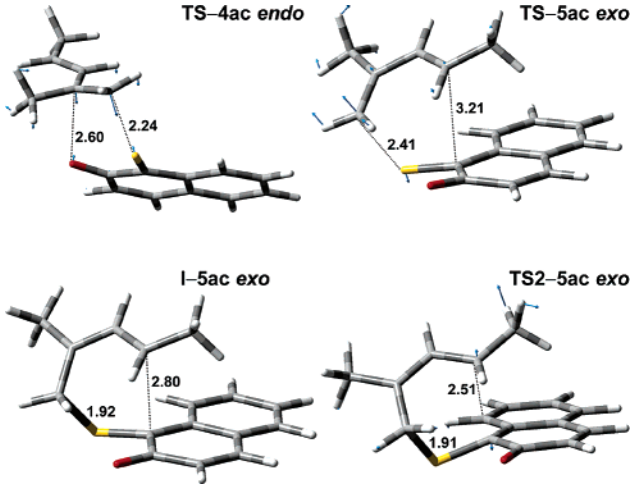

FIGURE 4. Transition states and intermediate for the reactions of **2a** and **3c**. Displacement vectors for each TS imaginary frequency are shown as blue arrows, and distances are reported in angstroms.

TABLE 2. Selected Distances (Å), Synchronicity Degrees $\Delta d_{TS/P}$, and Imaginary Frequencies (cm^{-1}) of the exo [2 + 4] TSs for the Reaction of *o*-TQs 2a−c with Dienes 3a−c

entry	S1−C2	C5−C6	$\Delta d_{TS}/P^a$	IF
TS-5aa	2.34	3.12	0.75	−133.823
TS-5ab	2.31	3.17	0.80	−144.987
TS-5ac	2.41	3.21	0.74	−108.734
TS-5ba	2.49	3.20	0.72	−61.0878
TS-5bb	2.43	3.22	0.77	−91.2803
TS-5ca	2.53	3.27	0.75	−54.9273
TS-5cb	2.46	3.29	0.80	−86.0762

[a] Products distances are provided in Table S4 (Supporting Information).

Supporting Information) and the visual inspection of the motion associated with imaginary frequencies show that all [4 + 2] cycloadditions take place along quite asynchronous transition states.

Indeed, as depicted in Figure 4 for the reaction **2a** + **3c**, the magnitude of the displacement vector associated with the forming C−S bond is larger than the one of the forming C−O bond and results are clear that the C−S bond formation foregoes the C−O. The $\Delta d_{TS/P}$ values range from 0.51 (**TS-4aa** and **TS-4ab**) to 0.62 (**TS-4ad** and **TS-4bc**), and the mean $\Delta d_{TS/P}$ value is a minimum (higher synchronicity) for [4 + 2] cycloadditions of *o*-TQ **2a** while a maximum (lower synchronicity) for *o*-TQ **2b**, probably due to the mesomeric electron-donating effect of the methoxyl group, which increases the negative charge over the quinonic oxygen (−0.234e, −0.250e, −0.230e for *o*-TQs **2a**, **2b** and **2c**, respectively, from Mulliken charges). Despite several attempts, only one TS was located for each [4 + 2] reaction, suggesting that the mechanism is fully concerted. On the other hand, the analysis of the geometrical parameters for [2 + 4] TSs (see Table 2) show that the reaction of *o*-TQs **2a**−**c** with dienes **3a**−**c** takes place in a strongly asynchronous or even unconcerted manner, with $\Delta d_{TS/P}$ values ranging from 0.72 (**TS-5ba**) to 0.80 (**TS-5ab** and **TS-5cb**). Moreover, two separate TSs, one for the formation of the C−S bond (**TS-5ac**, IF = −108.734 cm^{-1}) and the other for the formation of the C−C bond (**TS2-5ac**, IF = −123.688 cm^{-1}), and the stable intermediate **I-5ac** were located for the reaction of *o*-TQ **2a** with diene **3c**, thus supporting a stepwise mechanism for this example reaction (see Figure 4). To exclude any solvent influence on such a two-step mechanism, we reoptimized **TS-5ac**, **TS2-5ac**

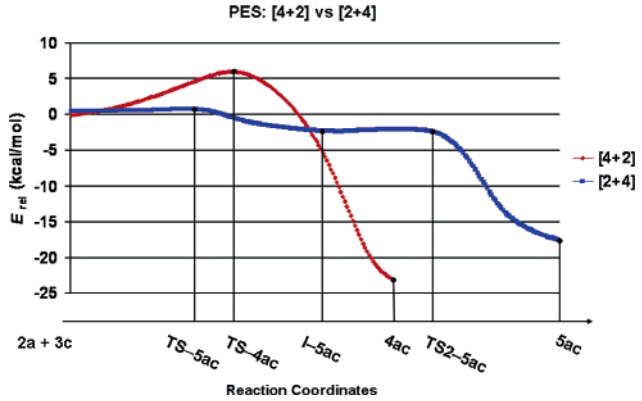

FIGURE 5. IRC analysis of the [4 + 2] and [2 + 4] reactions of *o*-TQ **2a** with diene **3c**.

and the intermediate **I-5ac** at the B3LYP/6-31G* level by including the solvent contribution ($CHCl_3$) by means of the PCM model, but analogue stationary points were located over the PES, as also confirmed by the vibrational analysis conduced at the same level of theory (see Figure S1 and Table S1, Supporting Information).

A further proof supporting the stepwise mechanism was found by performing extensive IRC analyses starting from both **TS-** and **TS2-5ac**: in the first case the reactants and the intermediate **I-5ac** were obtained in the reverse and forward directions, respectively, while product **5ac** (forward) and intermediate **I-5ac** (reverse) were obtained starting from **TS2-5ac**. An IRC analysis was also performed for the [4 + 2] cycloaddition of **2a** + **3c** starting from **TS-4ac**, confirming, in this case, a totally concerted reaction path as only reactants and product **4ac** were found as minima over the PES. The comparison of [4 + 2] and [2 + 4] IRCs is depicted in Figure 5, which graphically summarize the above statements. Moreover, it is worth noting that the energetic values and the geometrical parameters of TSs reported in Tables 1 and 2, S3, respectively, together with the IRC analyses depicted in Figure 5 show that, according to the Hammond's postulate, the [4 + 2] TSs are "late" (higher activation barrier, shorter lengths for the forming bonds) while the C−S [2 + 4] TSs occur at an "early" stage along the PES.

Unfortunately, despite the repeated trials, no intermediates nor TSs relative to the C−C bond formation were successfully located for the other [2 + 4] cycloadditions herein considered; thus, we cannot guarantee that all [2 + 4] reactions follow an unconcerted or a strongly asynchronous but concerted pathway. Indeed, as one can see from Figure 5 for **2a** + **3c**, the PES for the [2 + 4] cycloaddition was particularly flat in the region where the intermediates **I** and transition structures **TS2** should lie, making the localization of such stationary points extremely difficult for the current optimization algorithms. Moreover, repeated trials to perform IRC analyses starting from **TS-5aa** and **TS-5ab** provided the reactants in the reverse direction but failed in the forward direction at a point over the PES (after 64 and 63 steps of 0.1 $amu^{1/2}$ bohr from **TS-5aa** and **TS-5ab**, respectively) corresponding to geometries showing a fully formed C−S bond (1.92 Å for both structures) and a forming C−C bond (2.51 and 2.56 Å for **TS2-5aa** and **TS2-5ab**, respectively). Further optimizations did not fully converge either in the gas phase or in solution; however, vibrational analyses conduced on the last obtained IRC geometries revealed only one imaginary frequency corresponding to the stretching of the C−C forming bond.[29] The above observations suggest that the

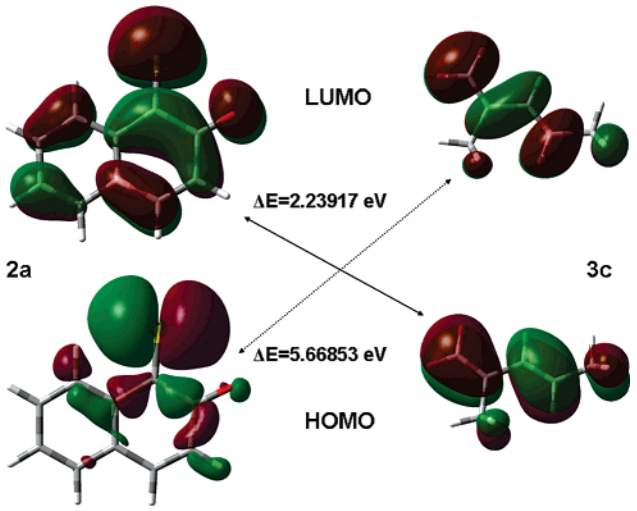

FIGURE 6. HOMO and LUMO for *o*-TQ **2a** and diene **3c**; the favored and symmetry-allowed interaction is $LUMO_{o-TQ}-HOMO_{1,3-diene}$.

TABLE 3. HOMO and LUMO Energies (eV) for *o*-TQs 2a−c and 1,3-Dienes 3a−f

entry	2a	2b	2c	3a	3b	3c	3d	3e	3f
LUMO	−3.95	−4.00	−4.10	−0.99	−1.03	−0.79	−0.74	−0.80	−0.93
HOMO	−6.46	−6.49	−6.44	−6.44	−6.49	−6.19	−6.13	−5.92	−5.93

IRC job failure could be due to the relevant change in the followed normal mode (IF = −133.823 and −144.987 cm^{-1} for **TS-5aa** and **TS-5ab**, IF = −167.426 and −156.155 cm^{-1} for the nonconverged **TS2-5aa** and **TS2-5ab**, respectively), thus enhancing the probability for two TSs to exist along the PES. It should be noted that such a change in the followed normal mode was not observed for "normal" concerted asynchronous reactions, such as the [4 + 2] cycloadditions described above. However, it should be also considered that even if the PES presents two TSs, as observed for the [2 + 4] reaction of **2a** + **3c**, the $\Delta H^{\ddagger}$ for the second step is quite negligible (0.2 kcal/mol for **TS2-5ac**) and thus the two reaction steps should occur within a decidedly narrow time range. For the above-mentioned reasons, we would prefer to consider the *o*-TQs [2 + 4] reaction mechanism as a borderline concerted asynchronous rather than unconcerted.

Regioselectivity. The frontier molecular orbitals depicted in Figure 6 for *o*-TQ **2a** and diene **3c**, together with HOMO and LUMO energies reported in Table 3, show that both the [4 + 2] and [2 + 4] cycloadditions of *o*-TQs **2a**−**c** with 1,3-dienes **3a**−**f** are controlled by the interaction of the LUMO of the *o*-TQs with the HOMO of the 1,3-diene. Thus, the [4 + 2] cycloadditions follow an inverse electron-demand pathway, as previously reported by Nair et al.,[8] while the [2 + 4] reactions formally follow a direct electron-demand pathway, as the *o*-TQ acts as the dienophile in [2 + 4] cycloadditions.

As depicted in Figure 7, the shape and the sign of the frontier molecular orbitals involved in the reaction show that both [4 + 2] and [2 + 4] cycloadditions could virtually provide two symmetry-allowed regioisomers, namely R1 and R2. Unless differently stated, the [4 + 2] R1 and R2 isomers derive from the energetically favored (and symmetry allowed) endo- and exo-TSs, respectively, while the exo-TSs were decidedly favored for both [2 + 4] R1 and R2 isomers (see Supporting Information for total energies). Concerning the [4 + 2] reaction of *o*-TQs **2a**−**c** with 1,3-diene **3c**, the R1 regioisomer is both kinetically

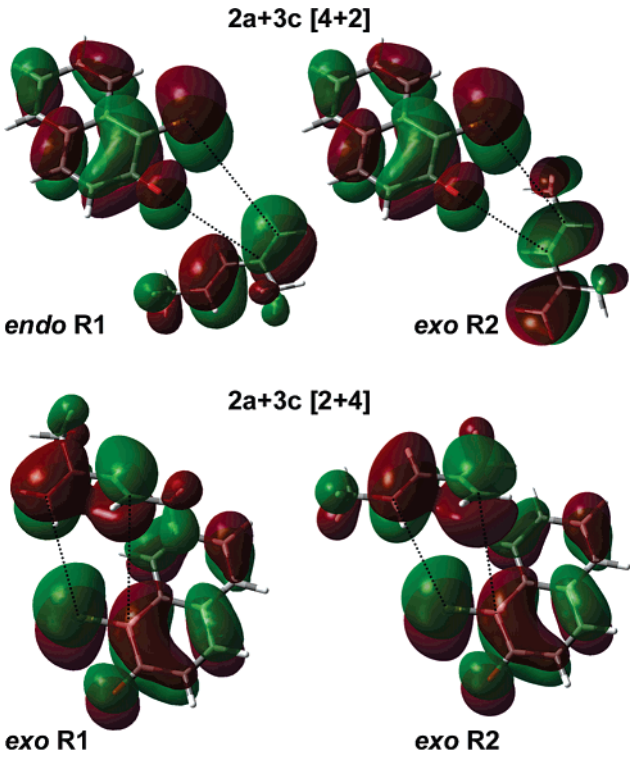

FIGURE 7. Symmetry-allowed $LUMO_{o-TQ}-HOMO_{1,3-diene}$ interactions for [4 + 2] and [2 + 4] paths.

and thermodynamically favored (see Table S5, Supporting Information), and thus, in perfect concordance with experimental results,[11] R1 is the only expected regioisomer. A different behavior was found for the reactions of *o*-TQs **2a**−**c** with the 2-methylbutadiene **3b**; indeed, in this case, R1 was kinetically favored by 0.4, 0.2, and 0.1 kcal/mol while R2 was thermodynamically favored with $\Delta\Delta H_{R2-R1}$ values of −1.6, −1.6, and −0.8 kcal/mol for **4ab**, **4bb**, and **4cb**, respectively. It should be noted that, as reported in our previous article, the reactions of **2a**−**c** with **3b** conduced under kinetic control did not afford products **4ab** and **4bb**, while traces of oxathiin **4cb** were actually observed by NMR.[11] The spectroscopic analysis of the raw reaction mixture, conduced on a 300 MHz instrument, led to the assignment of the R2 structure to compound **4cb**. Surprisingly, our theoretical results disagreed with the experimental findings previously reported, and such a discrepancy induced us to reconsider the reaction of thioquinone **2c** with diene **3b** by adopting thermodynamic conditions in order to enhance the formation of product **4cb** with respect to the spiro derivative **5cb** (see Supporting Information for experimental details). The ^{1}H NMR analysis performed with a 400 MHz spectrometer showed the formation of both regioisomers of product **4cb** with a ratio R1:R2 of 3:1, in good concordance with the predicted theoretical results. Concerning the [2 + 4] reactions, the available experimental results show that the spiro derivatives **5** were obtained as a mixture of R1 and R2 regioisomers whenever the asymmetric 1,3-dienes **3b,c** were employed.[11] Activation enthalpies reported in Table S5 show that the R1 isomer is kinetically favored for all the examples herein described, with $\Delta\Delta H^{\ddagger}_{R2-R1}$ values ranging from 0.6 (**5ab**, **5cb**) to 2.1 kcal/mol (**5ac**). For those compounds deriving from the 1,3-dimethylbutadiene **3c**, the more consistent $\Delta\Delta H^{\ddagger}_{R2-R1}$ values could be reasonably ascribed to the different steric hindrance on the diene carbon atom involved in the S−C bond formation. Indeed, in

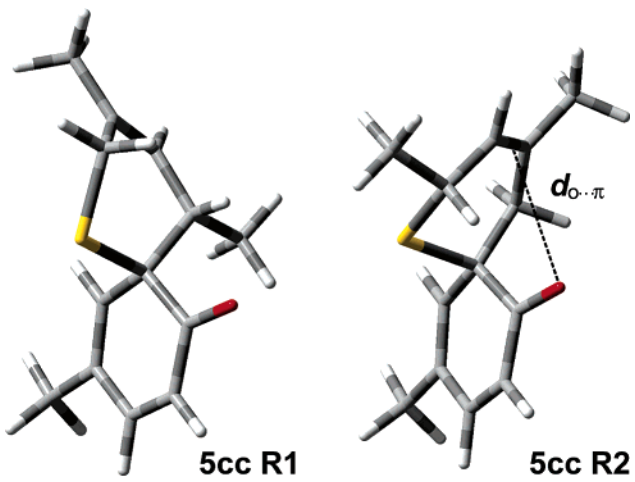

FIGURE 8. **5cc** regiosimers. Distances $d_{O\cdots\pi}$ (in Å) for products **5a**−**c** R2 isomers are 3.07 (**5ab**), 3.08 (**5ac**), 3.12 (**5bb**), 3.13 (**5bc**), 3.12 (**5cb**), 3.13 (**5cc**).

the case of R1, the S−C interaction occurs with the less substituted carbon while the opposite is observed for the least stable R2 regioisomer. On the other hand, reaction enthalpies ΔH show that the R2 regioisomer is always thermodynamically favored, as $\Delta\Delta H_{R2-R1}$ values resulted from −1.2 (**5bb**) to −4.1 kcal/mol (**5ac**)

The major thermodynamic stability of the R2 isomers could be ascribed to a favorable CH···O interaction between the C2−H and the O═C ($d_{H\cdots O}$ = 2.53 Å, C−H−O = 111.2° for compound **5cc**).[31] However, a CH···O interaction, involving the C4−H and the O═C could also be observed for R1 ($d_{H\cdots O}$ = 2.35 Å, C−H−O = 105.3°) and thus the lower R2 energy could be due to a dispersive interaction between the carbonyl oxygen and the C3−C4 double bond,[32] i.e., an O···π interaction that is not present in the R1 isomers, as represented in Figure 8. It is known that an O···π interaction between a phenyl group and the oxygen atom of an amidic carbonyl plays an important role in the target recognition of anhydrase II inhibitors,[33] and it is thus reasonable to think that O···π interactions could stabilize certain conformations of organic compounds. Indeed, the distances between the C3═C4 midpoint and the carbonyl oxygen ($d_{O\cdots\pi}$ in Figure 8) are comparable to those reported by literature for similar O···π interactions and, more generally, for nonbonding attractive interactions involving π systems.[34,35] It should be noted that the major R2 stabilization observed for compounds deriving from diene **3c** can be due to the unfavorable steric interaction between the carbocyclic ring and the C-5 linked methyl group, not present in diene **3b** derivatives. In conclusion,

(30) The convergence parameters obtained for **TS2-5aa** (**TS2-5ab**) are as follows: maximum force = 0.009772 (0.012569), rms force = 0.001951 (0.002374), maximum displacement = 0.112238 (0.123450), rms displacement = 0.027598 (0.030548), predicted change in energy = -2.411426×10^{-3} (-2.638542×10^{-3}). Restarting the optimization procedure did not produce relevant changes in geometry nor in energy.

(31) Desiraju, G. R. *Chem. Commun.* **2005**, 2995−3001.
(32) Dispersive interactions are long-range attractive forces, also known as London forces, due to instantaneous dipoles that arise during fluctuations in the electron clouds. Leach, A. R. *Molecular Modelling, Principle and Application*; Longman: Edinburg Gate, Harlow, 1996.
(33) Hunter, C. A.; Lawson, K. R.; Perkins, J.; Urch, C. J. *J. Chem. Soc., Perkin Trans. 2* **2001**, 651−669.
(34) Korenaga, T.; Tanaka, H.; Tadashi E.; Takashi, S. *J. Fluorine Chem.* **2003**, *122*, 201−205.
(35) Meyer, E. A.; Castellano, R. K.; Diederich, F. *Angew. Chem., Int. Ed.* **2003**, *42*, 1210−1250.

bearing in mind that spiro derivatives **5** are obtained mainly under kinetic conditions, the competitive kinetic and thermodynamic pathways calculated for the spiro derivatives **5** suggest that [2 + 4] reactions of *o*-TQs with asymmetric dienes would lead to mixtures of regioisomers, in concordance with the qualitative predictions based on the FMO theory (see Figure 7) as well as with the available experimental results.[11]

Conclusions

In this work we reported the first thorough study of the [4 + 2] and [2 + 4] cycloadditions of *o*-TQs and theoretical findings fit well with the available experimental results. We demonstrated that the [2 + 4] reactions are kinetically favored, but the resulting spiro derivatives **5** are less stable than the [4 + 2] oxathiinic products **4**, and thus under thermodynamic control the latter are the only isolable products. The analysis of the main geometrical parameters of TSs showed that, according with the Hammond's postulate, **TS-4** are "late", while **TS-5** are "early". Moreover, both reaction mechanisms were deeply analyzed by IRC calculations, evidencing a concerted asynchronous mechanism for [4 + 2] cycloadditions and a heavily asynchronous or even unconcerted mechanism for [2 + 4] cycloadditions. Finally, the strong regioselectivity of [4 + 2] reactions as well as the lack of regioselectivity observed for [2 + 4]s has been analyzed and explained.

Acknowledgment. Work carried out in the framework of the National Project: "Stereoselezione in Sintesi Organica. Metodologie ed Applicazioni" supported by the Ministero dell' Istruzione della Università e della Ricerca (MIUR), Roma. We thank the Centro Interuniversitario Lombardo per l'Elaborazione Automatica (CILEA) for computational facilities and the MIUR (FIRST) for financial support. Furthermore, we thank two anonymous referees for useful suggestions.

Supporting Information Available: Further computational details, extended tables, Cartesian coordinates, and energies of the mentioned stationary points. This material is available free of charge via the Internet at http://pubs.acs.org.

JO0604538